AD-A080 248 NAVAL OCEAN RESEARCH AND DEVELOPMENT ACTIVITY NSTL S--ETC F/G 8/10
THE NORDA/FLENUMOCEANCEN THERMODYNAMICAL OCEAN PREDICTION SYSTE--ETC(U)
NOV 79 R M CLANCY, P J MARTIN
UNCLASSIFIED NORDA-TN-54 NL

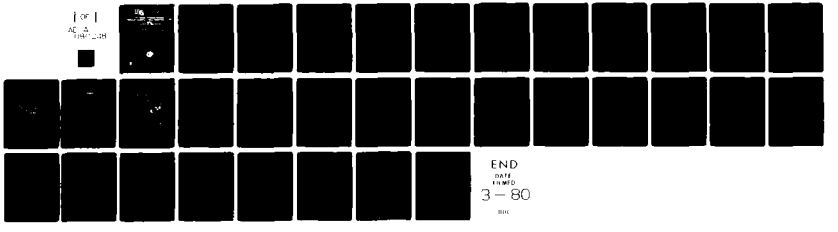

END
DATE FILMED
3-80
DTIC

LEVEL

(14) NORDA Technical Note 54

THE NORDA/FLENUMOCEANCEN THERMODYNAMICAL OCEAN PREDICTION SYSTEM (TOPS): A TECHNICAL DESCRIPTION.

(10) R. Michael Clancy
Paul J. Martin

Numerical Modeling Division
Ocean Science and Technology Laboratory

(11) November 1979 (12) 33

392773

NAVAL OCEAN RESEARCH AND DEVELOPMENT ACTIVITY
NSTL STATION, MISSISSIPPI 39529

LB

ABSTRACT

The Thermodynamical Ocean Prediction System (TOPS) is a general and flexible software framework for operational implementation of upper ocean forecast models at Fleet Numerical Oceanography Center (FLENUMOCEANCEN), Monterey, California. It was developed by NORDA Code 322 as a part of the Navy's Automated Environmental Prediction System (AEPS). TOPS is fully interfaced with the FLENUMOCEANCEN operational data base and meets all FLENUMOCEANCEN programming standards for operational programs. This technical note discusses the uses for TOPS, provides documentation of the physics currently represented in the system, indicates probable future developments, and briefly addresses the problem of forecast verification.

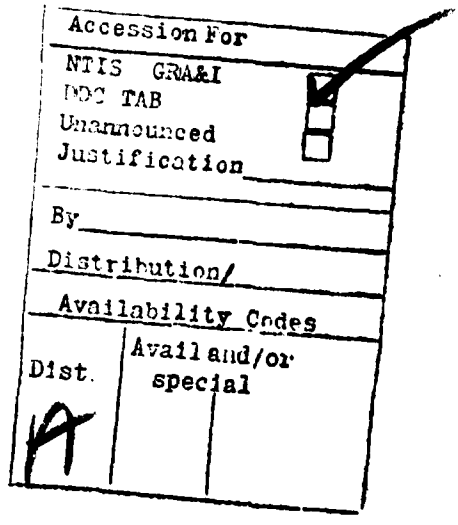

CONTENTS

ILLUSTRATIONS

TABLES

I. INTRODUCTION

Almost universally, the upper ocean is characterized by a mixed-layer extending from the surface to about 5-100 m depth,in which temperature and salinity exhibit only small changes with depth. In addition to having important implications for long-range weather prediction, climate modeling, fisheries operations, ocean thermal energy conversion and pollution control, the depth and stratification of this layer have important impacts on the propagation of underwater sound. Thus, synoptic knowledge of the structure of the oceanic mixed layer is of great interest to the Navy.

The mixed-layer owes its high degree of vertical uniformity to mixing caused by turbulence that is generated by shear instabilities, breaking waves, and surface cooling. A dynamically stable water mass in which the vertical eddy fluxes are extremely small usually exists below the mixed-layer.

During periods of strong wind forcing and/or strong surface cooling, the mixed-layer tends to deepen because water is entrained into the layer from below by turbulent mixing. During periods of relatively weak wind forcing and/or strong surface heating, however, the source of turbulent kinetic energy may become too weak to maintain active entrainment at the base of the mixed-layer, causing the layer to retreat to a shallower depth. In this way, the thermal structure of the mixed-layer is modified substantially on time scales of a few days by the passage of atmospheric disturbances (e.g., Elsberry and Camp, 1978; Elsberry and Raney 1978). Hence, the temporal variability of the thermal structure of the upper ocean is much larger than that of the region in and below the main thermocline.

Modeling of the oceanic mixed-layer is intrinsically linked to parameterization of turbulent processes and, consequently, is a difficult problem. Over the past decade, however, tremendous interest has been shown in upper ocean modeling and much progress has been made. For example, even though much is still unknown about the fundamental nature of turbulence, field data have shown the state of the mixed-layer to be highly predictable with a variety of turbulence parameterization models. As a result, it is now reasonable to expand the realm of mixed-layer modeling from the experimental domain to the operational domain by constructing upper ocean forecast systems that are interfaced with operational data bases. The Thermodynamical Ocean Prediction System (TOPS), developed for Fleet Numerical Oceanography Center (FLENUMOCEANCEN) by NORDA Code 322, is the first such system. TOPS is regarded as a component of the Navy's steadily evolving Automated Environmental Prediction System (AEPS).

Several important uses for TOPS are anticipated. For example, it can be used to improve the daily Fleet Numerical Ocean Thermal Structure Analysis (which provides initial conditions for the forecast model) by producing a 24-hour forecast for use as the first-guess field (i.e., the best estimate of the analyzed field before new data is assimilated) in the following day's analysis. In this way, the results predicted by the forecast model are fed back into the analysis on a daily basis. This should improve the analysis everywhere by tending to make it dynamically consistent with the atmospheric forcing, which presumably, is known fairly well. The improvement should be especially large in data-sparse regions where, in the absence of a forecast model, the analyzed thermal field is constrained to stay very near climatology, regardless of the local atmospheric forcing.

In addition to requiring knowledge of the instantaneous thermodynamical state of the upper ocean, the Navy needs to have the capability to forecast this state

over periods of several days, as this ability could be tactically significant. For example, the solar heating cycle modifies the stratification of the upper ocean in an acoustically important way, but this information is obviously not resolved by the daily analysis. Furthermore, intense, rapidly moving meteorological disturbances, such as extratropical cyclones and their associated warm and cold fronts, can substantially modify the upper ocean over vast areas during a period of 72 hours. Given proper initial conditions and a reasonably accurate 72-hour weather prediction, TOPS can provide a useful 72-hour forecast of the response of the upper ocean to these forcing mechanisms.

The following section gives a detailed description of the physics represented in the present configuration of TOPS. Section III summarizes the system and its uses, gives a limited view of probable future developments, and comments briefly on the problem of forecast verification.

II. PRESENT CONFIGURATION OF TOPS

Two separate forecast models are available in the present configuration of TOPS: a non-advective or "quasi-one-dimensional" model and an advective or "quasi-three-dimensional" model. Both models use the same parameterizations, grid, initial conditions, and upper and lower boundary conditions.

A. PROGNOSTIC EQUATIONS FOR THE NON-ADVECTIVE MODEL (HMLMS)

In the non-advective forecast model or Hemispheric Mixed Layer Model System (HMLMS), planetary rotation and the convergence of vertical eddy and radiative fluxes are assumed to be the only processes controlling the dynamics of the upper ocean. Under these assumptions, the conservation equations for temperature, salinity, and momentum are

$$\frac{\partial \bar{T}}{\partial t} = \frac{\partial}{\partial z}\left(\overline{-w'T'} + \nu\frac{\partial \bar{T}}{\partial z}\right) + \frac{1}{\rho_w c}\frac{\partial \bar{F}}{\partial z}\,, \tag{1}$$

$$\frac{\partial \bar{S}}{\partial t} = \frac{\partial}{\partial z}\left(\overline{-w'S'} + \nu\frac{\partial \bar{S}}{\partial z}\right) \tag{2}$$

$$\frac{\partial \bar{u}}{\partial t} = f\bar{v} + \frac{\partial}{\partial z}\left(\overline{-w'u'} + \nu\frac{\partial \bar{u}}{\partial z}\right) - D\bar{u}\,, \tag{3}$$

$$\frac{\partial \bar{v}}{\partial t} = -f\bar{u} + \frac{\partial}{\partial z}\left(\overline{-w'v'} + \nu\frac{\partial \bar{v}}{\partial z}\right) - D\bar{v}\,, \tag{4}$$

where T is the temperature, S the salinity, u and v the x- and y-components of the current velocity (x and y relative to the grid, see Section II.E), w the z-component of current velocity, F the downward flux of solar radiation, D a damping coefficient, ν a diffusion coefficient, f the Coriolis parameter, t the time and z the vertical coordinate (positive upward). Spatial averages over a region defined by a cell in the horizontal mesh are denoted by $(\bar{\ })$ and primes indicate departure from these averages. Thus, for example, the quantity $\overline{w'S'}$ represents the vertical eddy (i.e., turbulent) flux of salinity.

The terms involving the damping coefficient D in (3) and (4) represent the drag force caused by the stress at the base of the mixed-layer associated with the propagation of internal wave energy away from the wind-forced region (e.g., Pollard and Millard, 1970). As discussed by Niiler and Kraus (1977), this drag

force can contribute to the relatively fast attenuation of inertial oscillations observed in the mixed-layer. We use the value $D = 0.1\ day^{-1}$, which is within the range of estimates for this quantity.

The terms involving ν in (1)-(4) represent very weak "background" eddy diffusion that exists even below the mixed-layer. We set $\nu = 1\ cm^2\ s^{-1}$ and note that, on time scales less than one month, the model is not sensitive to the value of ν, provided that it is not zero.

Equations (1)-(4) are solved on a three-dimensional grid in order to produce a three-dimensional forecast of the state of the upper ocean. Since there are no horizontal processes considered in this formulation, however, it is best thought of as a "quasi-one-dimensional" model.

Over most of the world ocean, purely one-dimensional mixing processes account for a major portion of the upper ocean's response to strong atmospheric forcing (e.g., Camp and Elsberry, 1978). Hence, even though this quasi-one-dimensional formulation is quite simple, it should be capable of representing a significant part of the upper ocean's short time scale response, provided that suitable parameterizations of the vertical eddy fluxes are used.

B. PROGNOSTIC EQUATIONS FOR THE ADVECTIVE MODEL (AHMLMS)

In the advective forecast model or Advective Hemispheric Mixed Layer Model System (AHMLMS), horizontal and vertical advection and horizontal diffusion of temperature and salinity are included in addition to the radiative and vertical mixing processes of the non-advective model (see Section II.A). As a result, the conservation equations for temperature and salinity become

$$\frac{\partial \overline{T}}{\partial t} = \frac{\partial}{\partial z}\left(\overline{-w'T'} + \nu\frac{\partial \overline{T}}{\partial z}\right) + \frac{1}{\rho_w c}\frac{\partial \overline{F}}{\partial z} \tag{5}$$

$$- \frac{\partial}{\partial x}(u_a\overline{T}) - \frac{\partial}{\partial y}(v_a\overline{T}) - \frac{\partial}{\partial z}(w_a\overline{T}) + A\left(\frac{\partial^2\overline{T}}{\partial x^2} + \frac{\partial^2\overline{T}}{\partial y^2}\right),$$

and

$$\frac{\partial \overline{S}}{\partial t} = \frac{\partial}{\partial z}\left(\overline{-w'S'} + \nu\frac{\partial \overline{S}}{\partial z}\right) \tag{6}$$

$$- \frac{\partial}{\partial x}(u_a\overline{S}) - \frac{\partial}{\partial y}(v_a\overline{S}) - \frac{\partial}{\partial z}(w_a\overline{S}) + A\left(\frac{\partial^2\overline{S}}{\partial x^2} + \frac{\partial^2\overline{S}}{\partial y^2}\right),$$

where u_a, v_a and w_a are the x-, y-, and z-components of the advection current and A is a horizontal eddy diffusion coefficient ($A = 10^8\ cm^2\ s^{-1}$). Definitions of the remaining symbols can be found either in Section II.A or in the Appendix.

Horizontal pressure gradients and horizontal advection and diffusion are neglected in the momentum equations in the advective model. Therefore, these equations still take the form of Equations (3) and (4) of the non-advective model.

Equations (3) and (4) can be used to determine the Ekman component of the advection current. Since there are no pressure gradient terms in (3) and (4), however, they cannot be used to determine the geostrophic component. Therefore, even though advection and diffusion of temperature and salinity occur in three dimensions in this formulation, it is not a true three-dimensional model. It is, perhaps, best termed a "quasi-three-dimensional" model.

At present, the geostrophic component of the advection current is calculated diagnostically from a climatological data base (see Section II.H.2). In future applications, the geostrophic current will be provided by a hydrodynamical model with high horizontal resolution.

As mentioned in the previous section, one-dimensional mixing and radiative processes dominate the dynamics of the mixed-layer on time scales of a few days over most of the world's oceans. On longer time scales, however, advective processes can make important contributions to the heat and salinity budgets of the upper ocean. Therefore, assuming that it is supplied with realistic advection currents, the advective model should perform better than the non-advective model on long time scales.

The advective model will be installed on the CYBER 203 computer at FLENUMOCEANCEN in 1981 and will become the primary operational model in TOPS. The non-advective model is currently operative on the CYBER 175 at Monterey. Even after the advective model becomes operational, the non-advective version will remain active by serving as back-up model to be run on the CYBER 175 in the event that the CYBER 203 is down. This back-up capability will help guarantee the operational availability of the product fields generated by TOPS.

C. PARAMETERIZATION OF TURBULENT MIXING

The Level-2 turbulence closure theory of Mellor and Yamada (1974) is currently used to parameterize the vertical eddy fluxes of temperature, salinity and momentum in both the advective and non-advective models. In this parameterization, the fluxes are given by

$$\overline{w'T'} = -\ell q S_H \frac{\partial \bar{T}}{\partial z} \equiv -K_H \frac{\partial \bar{T}}{\partial z} , \tag{7}$$

$$\overline{w'S'} = -\ell q S_H \frac{\partial \bar{S}}{\partial z} \equiv -K_H \frac{\partial \bar{S}}{\partial z} , \tag{8}$$

$$\overline{w'u'} = -\ell q S_M \frac{\partial \bar{u}}{\partial z} \equiv -K_M \frac{\partial \bar{u}}{\partial z} , \tag{9}$$

and

$$\overline{w'v'} = -\ell q S_M \frac{\partial \bar{v}}{\partial z} \equiv -K_M \frac{\partial \bar{v}}{\partial z} , \tag{10}$$

where K_H and K_M are eddy diffusion coefficients, ℓ is the turbulence length scale, q is the square root of twice the turbulent kinetic energy, and S_H and S_M are functions of the gradient Richardson number Ri, where

$$Ri \equiv \frac{-\frac{g}{\rho_w}\frac{\partial \bar{\rho}}{\partial z}}{\left[\left(\frac{\partial \bar{u}}{\partial z}\right)^2 + \left(\frac{\partial \bar{v}}{\partial z}\right)^2\right]} . \tag{11}$$

Here, g is the acceleration of gravity and ρ is the mean-field density calculated from $\bar{T}$ and $\bar{S}$ according to the equation of state proposed by Freidrich and Levitus (1972).

The functional forms for S_H and S_M are derived by Mellor and Yamada (1974) and require specification of three empirical constants. These constants, however, are determined once and for all from neutrally stratified turbulent flow data. The resulting curves for S_H and S_M are shown in Figure 1. Note the implied cutoff of turbulence at Ri = 0.23.

The quantity q is calculated from a form of the turbulent kinetic energy equation that expresses a local balance of shear production, buoyancy production, and viscous dissipation of turbulent kinetic energy

$$\ell q S_M \left[\left(\frac{\partial \bar{u}}{\partial z} \right)^2 + \left(\frac{\partial \bar{v}}{\partial z} \right)^2 \right] + \ell q S_H \left(\frac{g}{\rho_w} \frac{\partial \bar{\rho}}{\partial z} \right) - \frac{q^3}{15\ell} = 0 \tag{12}$$

where (7)-(10) and the equation of state have been used. Hence, the basic assumption of this turbulence model is that transports of turbulent kinetic energy can be neglected.

Finally, we follow Mellor and Durbin (1975) and calculate the turbulence length scale from the ratio of the first to the zeroth moment of the turbulence field

$$\ell = \frac{0.1 \int_{-\infty}^{0} |z| q dz}{\int_{-\infty}^{0} q dz} . \tag{13}$$

This equation, plus (7)-(12), closes the turbulence parameterization. This turbulence model has been applied to the oceanic mixed-layer with success by Mellor and Durbin (1975), Martin (1976), Martin and Roberts (1977), Martin and Roberts (1978), Clancy (1979), Martin and Thompson (1980), and Warn-Varnas et al. (1980). It has been compared to higher-order turbulence closure models with favorable results by Mellor and Yamada (1974) and Warn-Varnas and Piacsek (1979).

D. PARAMETERIZATION OF THE EXTINCTION OF SOLAR RADIATION

Although only a small amount of the incident solar radiation penetrates below the upper few meters of the sea (about 70% is absorbed in the upper 5 m, Jerlov, 1968), the penetration of solar radiation can affect mixed-layer dynamics and the density structure of the upper ocean in several ways.

1. Penetration of solar radiation provides a means of warming the region below the mixed-layer where vertical diffusion of heat is relatively weak. This process is especially effective when the mixed-layer is shallow.

2. Penetration of solar radiation allows for a higher level of turbulent kinetic energy within the mixed-layer. Since less heat has to be mixed downward, less turbulent kinetic energy is absorbed by potential energy production. This can result in weaker stability at the base of the mixed-layer and a deeper mixed-layer.

3. Penetration of solar radiation allows convection to occur between the surface and the compensation depth when the loss of heat at the surface is less than the absorption of solar radiation. The compensation depth is defined as the depth above which the amount of solar radiation absorbed by the sea is equal to the loss of heat from the surface. Convection can occur due to the upward flux of heat from the region above the compensation depth to the surface.

The extinction rate of solar radiation used in TOPS is from Jerlov (1968). Table I lists the percentage of solar radiation that penetrates to certain

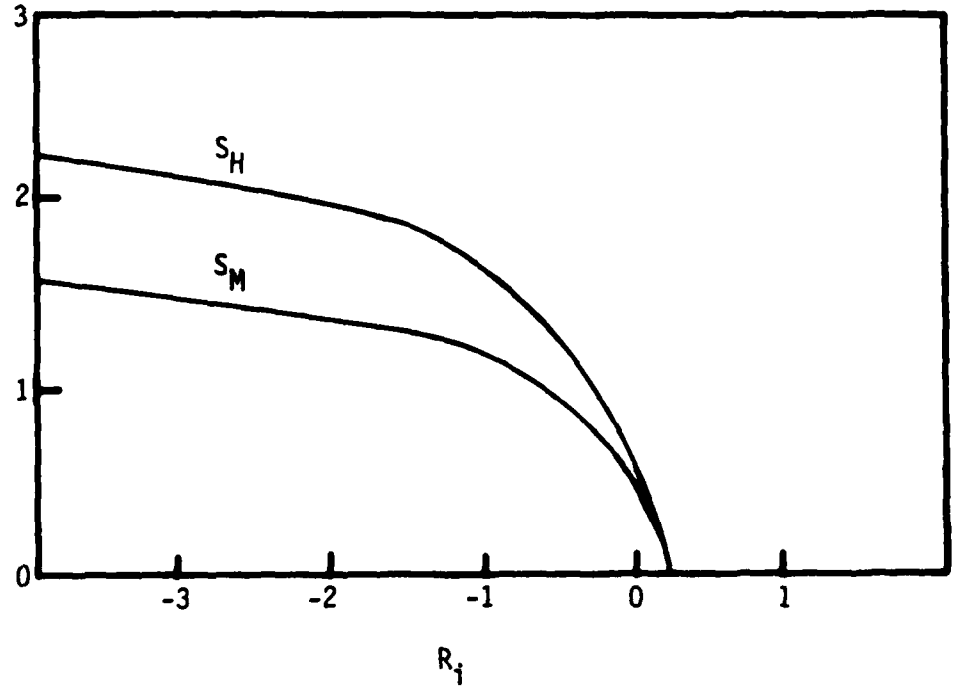

Figure 1. The stability functions S_H and S_M as a function of gradient Richardson number R_i.

depths for several types of water in the open ocean. The water types are classified according to their optical clarity from Type I for very clear ocean water to Type III for fairly turbid ocean water such as might be found in a biologically productive region. Figure 2 shows the worldwide distribution of the various water types.

The divergence of the solar radiative flux in TOPS is calculated from

$$\frac{\partial F}{\partial z} = F_o \frac{d\gamma}{dz} \tag{14}$$

where F_o is the total solar radiation penetrating the surface and γ is the fraction of F_o penetrating to a depth z. The quantity γ is interpolated from the data in Table 1.

TOPS currently employs an extinction profile for Type IA (clear) ocean water, which is (according to Figure 2) the most common type in the open ocean. However, plans are to amend the system to account for regional and perhaps seasonal differences in water type according to Figure 2 and more recent data.

E. GRID

The vertical grid used in both the advective and non-advective models consists of 17 levels between the surface and 500 m depth and is shown in Figure 3. High resolution is achieved near the surface in order to properly resolve the mixed-layer, and every fixed level in the FLENUMOCEANCEN Expanded Ocean Thermal Structure (EOTS) analysis is represented in this grid. Note that the vertical eddy fluxes and w_a are defined at depths midway between those for which temperature, salinity, and momentum are defined.

For the horizontal representation in both models, $\bar{T}$, $\bar{S}$, $\bar{u}$ and $\bar{v}$ are defined at the points of the standard FLENUMOCEANCEN 63 X 63 Northern Hemisphere Polar Stereographic Grid (see Figure 4). This grid is true at 60°N where the spacing is 381 km.

In the advective model, w_a is also defined on this grid, but u_a and v_a are staggered with respect to these points. Figure 5 shows the basic elements of the resulting grid system. Note that in both model formulations, the x- and y-directions are taken relative to the grid, not the earth.

F. INITIAL CONDITIONS

The initial temperature field is taken from the daily ocean thermal structure analysis produced by the FLENUMOCEANCEN Operational System. TOPS can accept input from either the Expanded Ocean Thermal Structure (EOTS) analysis system or the older Ocean Thermal Structure (OTS) analysis system.

These analysis schemes contain no explicitly modeled physics and are based entirely on standard information blending concepts. The daily Northern Hemisphere data set input to these systems consists of about 200 XBT observations, 2000 bucket sea-surface temperature observations, and 20,000 satellite sea-surface temperature observations from TIROS-N. Since information is blended vertically as well as horizontally, the sea-surface temperature observations contribute information to the subsurface thermal analysis. In data-sparse regions, the analyzed thermal field remains very near a state determined by a daily interpolation of monthly climatology. This monthly climatology is based on an

TABLE 1

PERCENTAGE OF TOTAL SURFACE IRRADIANCE PENETRATING TO A GIVEN DEPTH FOR A SOLAR ALTITUDE OF 90° (from Jerlov, 1968)

	Oceanic Water				
Depth (m)	I	IA	IB	II	III
0	100.0	100.0	100.0	100.0	100.0
1	44.5	44.1	42.9	42.0	39.4
2	38.5	37.9	36.0	34.7	30.3
5	30.2	29.0	25.8	23.4	16.8
10	22.2	20.8	16.9	14.2	7.6
20					
25	13.2	11.1	7.7	4.2	0.97
50	5.3	3.3	1.8	0.70	0.041
75	1.68	0.95	0.42	0.124	0.0018
100	0.53	0.28	0.10	0.0228	
150	0.056			0.00080	
200	0.0062				

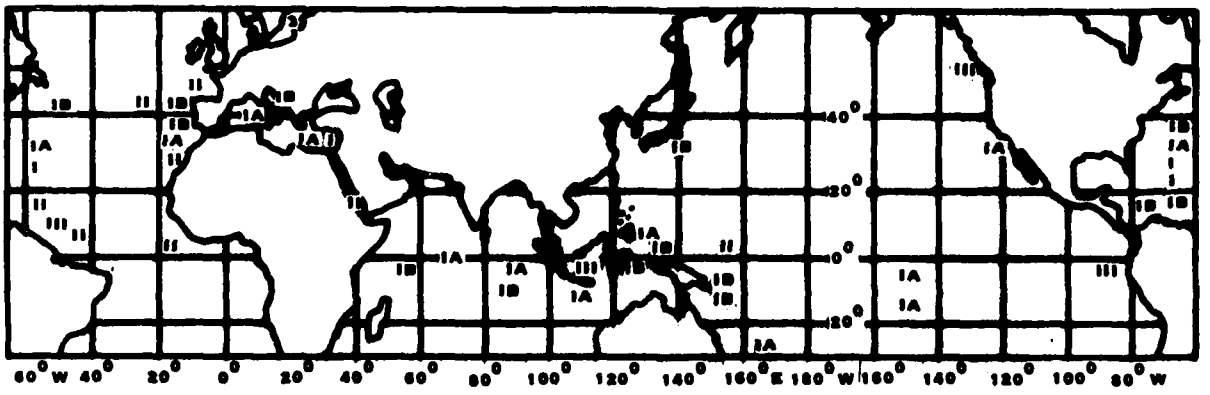

Figure 2. Regional distribution of optical water types (from Jerlov, 1968).

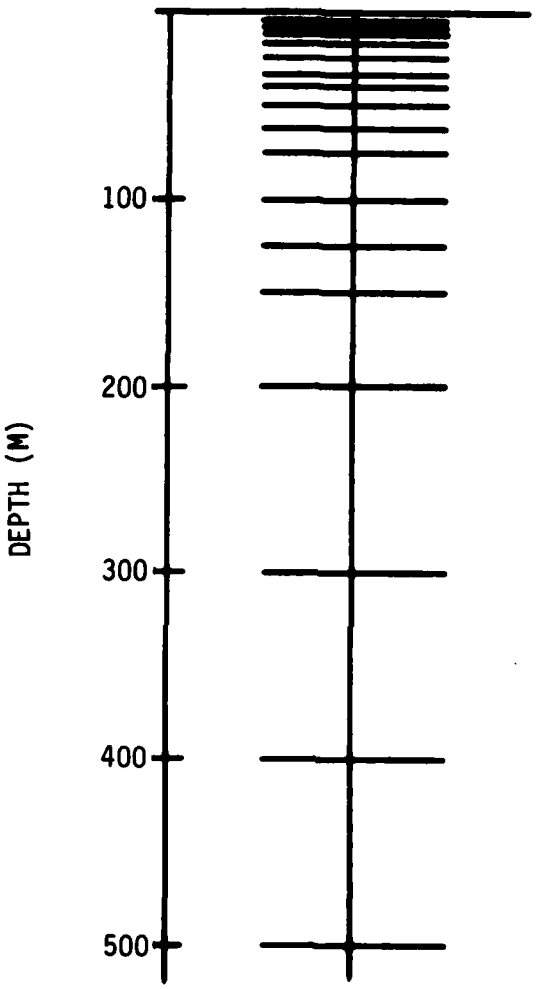

Figure 3. Vertical grid utilized by TOPS. The quantities $\overline{T}$, $\overline{S}$, $\overline{u}$, $\overline{v}$, u_a and v_a are defined at the depths indicated in the figure. All turbulence quantities and w_a are defined at depths midway between those shown in the figure.

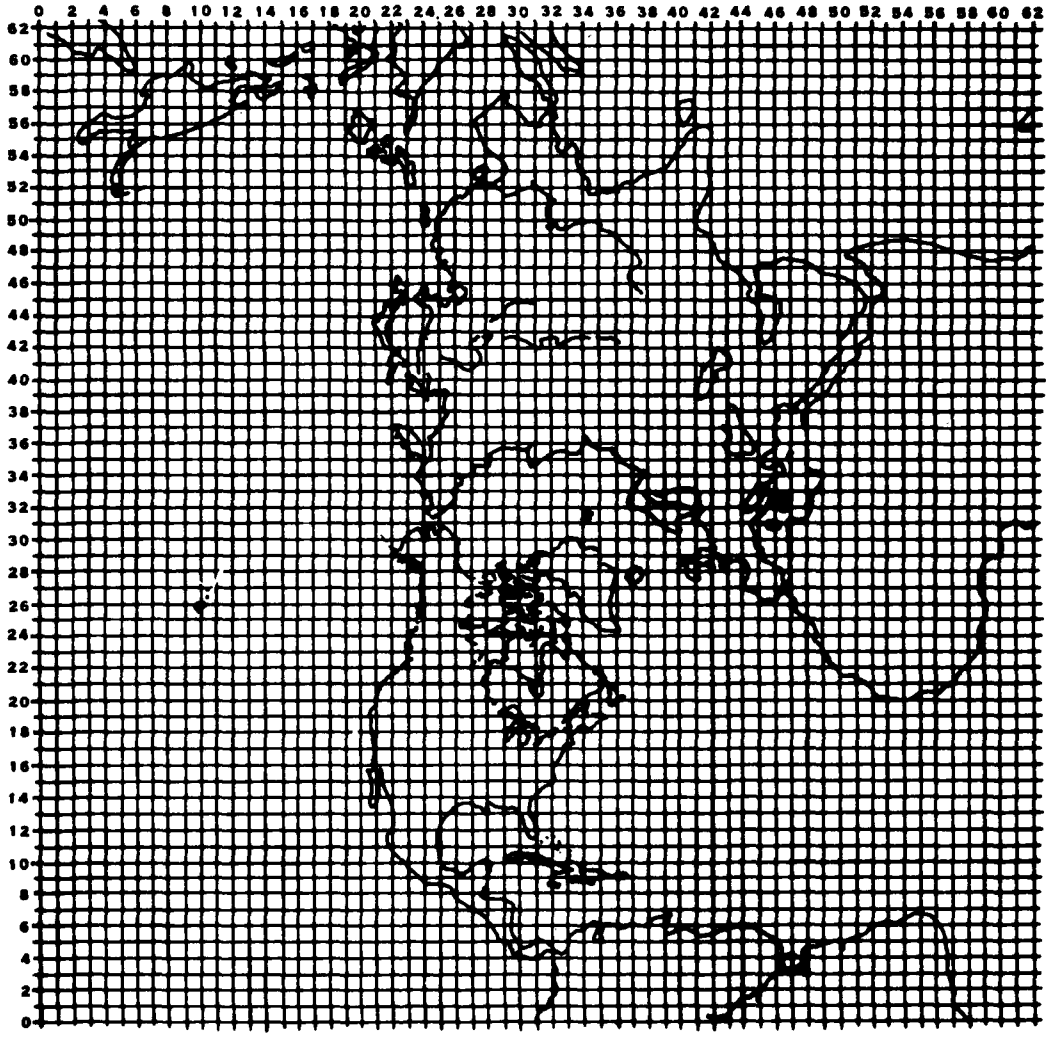

Figure 4. Standard FLENUMOCEANCEN 63 x 63 Northern Hemisphere Polar Stereographic Grid on which $\overline{T}$, $\overline{S}$, $\overline{u}$, $\overline{v}$, and w_a are defined.

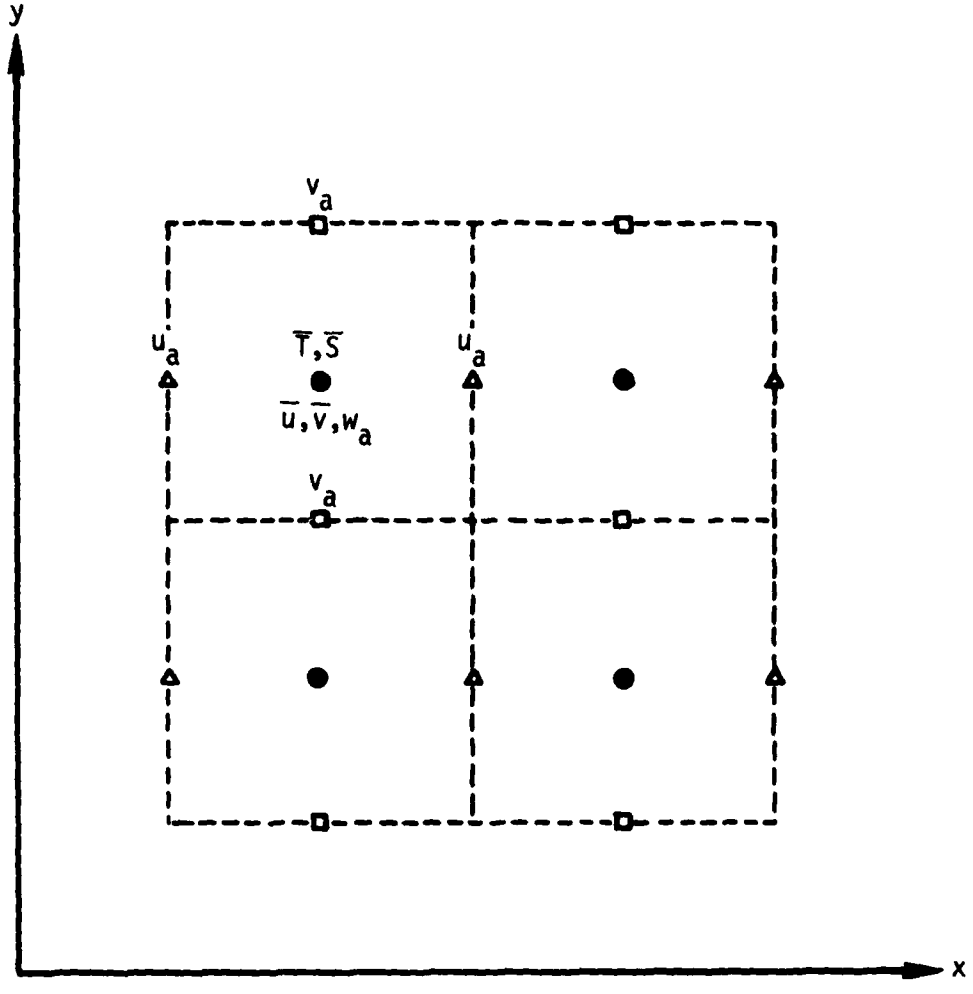

Figure 5. Staggered grid system used in the advective model. The quantities $\bar{T}$, $\bar{S}$, $\bar{u}$, $\bar{v}$, and w_a are defined at the points denoted ●, which correspond to the points in the standard FLENUMOCEANCEN 63 x 63 Northern Hemisphere Polar Stereographic Grid. The quantity u_a is defined at points denoted by △, and v_a is defined at points denoted by □. The interpolated climatological density field and the geostrophic stream function are defined at the corners of the dashed-line boxes.

objective analysis of approximately 600,000 bathythermograph observations made in the northern hemisphere prior to 1974 (see Weigle and Mendenhall, 1974).

At present, the first-guess field for each day's analysis is generated from the previous day's analysis by a forecast of persistence, plus adjustment toward the daily interpolated climatology. As mentioned in Section I, TOPS will eventually be used to generate the first-guess field, and thereby bring physics into the analysis by tending to make it dynamically consistent with the atmospheric forcing. See Holl et al. (1979) for a detailed discussion of the mathematical techniques currently used in the analysis schemes.

The initial salinity field is taken from a daily interpolation of monthly climatology. Inclusion of salinity in the forecast models is necessary, since it makes an important contribution to the density stratification in some regions and thereby affects the vertical turbulent mixing. Lack of a synoptic analysis for salinity, however, can present a problem in a few areas. For example, anomalous (i.e., non-climatological) salinity distributions can sometimes allow strong temperature inversions to exist at the base of the mixed-layer in high latitudes. If such an inversion is picked up by the daily ocean thermal structure analysis, then an unrealistic convective adjustment will occur in the model at that location. Use of temperature-salinity (T-S) relationships is not an adequate solution to this problem, since these relationships cannot be applied with confidence to the mixed-layer in these anomalous regions.

To overcome the problem, an option exists in TOPS which allows the salinity to be adjusted slightly from climatology in order to guarantee that: (1) the initial density stratification below the mixed-layer does not fall below some user-specified minimum value, and (2) the initial vertical gradient of density in the mixed-layer for a forecast performed on day N is given by the 24 hour forecast vertical density gradient in the mixed-layer calculated on day N-1. To <u>begin</u> a sequence of daily forecast runs, the salinity is adjusted to make the initial density stratification neutral in the mixed-layer.

The initial momentum field is also provided by carrying information forward in time from day to day. To begin a sequence of daily forecast runs, the initial momentum profile is set to zero below the base of the mixed-layer and taken to vary linearly in the mixed-layer such that the mixed-layer-averaged flow is equal to the vertically averaged Ekman drift. In successive forecast runs, however, the initial momentum field is given by the 24 hour forecast momentum field calculated by the previous day's run.

The turbulence length scale ℓ (see Section II.C) is initialized in a similar manner. To begin a sequence of forecast runs, ℓ is set to 2.5 m. In subsequent forecast runs, ℓ is provided by the value produced by the 24 hour forecast of the previous day's run.

Note that with the initial conditions supplied in the manner described above, the turbulent kinetic energy, the vertical eddy diffusion coefficients, the vertical eddy flux of momentum, and the vertical eddy flux of density (to the approximation that a linear equation of state holds) are conserved in the process of updating the model-predicted temperature field with the daily ocean thermal structure analysis (see Section II.C). This treatment tends to make the initial state consistent with both the atmospheric forcing and the dynamics of the turbulence parameterization model, which lessens the "initialization shock" associated with bringing the temperature observations into the model each day via the daily analysis, and restarting the forecast.

G. BOUNDARY CONDITIONS

The upper boundary conditions for the temperature, salinity, and momentum conservation equations are provided by surface fluxes that are forecast, out to a period of 72 hours on the same grid used by TOPS, by operational FLENUMOCEANCEN atmospheric models. Thus,

$$\left[\overline{-w'T'} + \nu\frac{\partial\overline{T}}{\partial z}\right]_{z=0} = \frac{-(B_o + H_o + LQ_o)}{\rho_w c}, \tag{15}$$

$$\left[\overline{-w'S'} + \nu\frac{\partial\overline{S}}{\partial z}\right]_{z=0} = \frac{(Q_o - P_o)\overline{S}_o}{\rho_w}, \tag{16}$$

$$\left[\overline{-w'u'} + \nu\frac{\partial\overline{u}}{\partial z}\right]_{z=0} = \frac{\tau^x}{\rho_w}, \tag{17}$$

$$\left[\overline{-w'v'} + \nu\frac{\partial\overline{v}}{\partial z}\right]_{z=0} = \frac{\tau^y}{\rho_w}, \tag{18}$$

where B_o is the surface infrared radiative flux, H_o is the surface sensible heat flux, LQ_o is the surface latent heat flux, P_o is the surface precipitation rate, S_o is the surface salinity, and τ^x and τ^y are the components of the surface wind stress. Definitions for the remaining symbols can be found in either earlier sections or in the Appendix.

The components of the surface wind stress are computed at 6 hour intervals from

$$\tau^x = \rho_a C_D U(U^2 + V^2)^{\frac{1}{2}}, \tag{19}$$

and

$$\tau^y = \rho_a C_D V(U^2 + V^2)^{\frac{1}{2}}, \tag{20}$$

where U and V are the x- and y-components of the 6-hourly available wind velocity vector at a reference level above the sea surface, ρ_a is a reference density for air, and C_D is a constant drag coefficient. The resulting components of the wind stress and the quantities $(B_o + H_o + LQ_o)$ and Q_o, which are also derived from the FLENUMOCEANCEN fields at 6 hour intervals, are then interpolated to each time step (0.5 hour) of the forecast models. At present, only a simple linear interpolation scheme is used. However, a higher order interpolation scheme will be adopted in the future, if it proves warranted.

The surface precipitation rate P_o is derived from a predicted field of 12 hour accumulated precipitation. It is simply assumed constant during each 12 hour period of the forecast.

The surface solar radiation flux F_o (which provides the upper boundary condition for the radiational heating calculation) is available from the atmospheric model only at 6 hour intervals. It is interpolated to each time step of the oceanic models according to

$$F_o = I\cos\alpha \tag{21}$$

where α is the time-varying local zenith angle of the sun and I is a linear function of time chosen such that the resulting curve for F_o passes through all of the 6-hourly available values. This treatment is necessary to allow adequate representation of the solar flux.

The studies of Johnson (1977), Paulus (1978) and Elsberry et al. (1979) have indicated that the wind stress and heat flux fields derived from the FLENUMOCEANCEN operational system do provide fairly realistic synoptic time scale forcing parameters for ocean prediction. However, problem areas, where the integrated surface heat flux is not consistent with the change in the heat content of the upper ocean derived from observations, have been identified (see Elsberry et al., 1979). This difficulty seems to be most severe south of latitude 30° and is probably related to the fact that the present atmospheric model is only hemispheric in coverage. Implementation of the Naval Operational Global Atmospheric Prediction System (NOGAPS) will probably improve the surface flux fields in this region considerably.

The lower boundary conditions for the conservation equations are provided by holding the temperature, salinity, and momentum constant at the lower boundary of the model during each forecast run. The temperature and salinity are defined there by a linear extrapolation of the initial conditions downward below 400 m. The momentum field at the bottom boundary is always set to zero.

Because there are no horizontal exchanges of heat and salinity in the non-advective model, no lateral boundary conditions are required in that formulation. In the advective model, the normal component of the advection current and the normal derivatives of $\bar{T}$ and $\bar{S}$ are taken to be zero at land-sea boundaries. Thus, no advection or diffusion of heat or salinity is allowed across these boundaries. In addition, the normal derivatives of $\bar{T}$ and $\bar{S}$ on the outer boundary surrounding the forecast domain (i.e., one-half grid space outside of the 63 X 63 grid) are assumed to be zero, which implies no diffusion of heat and salinity into or out of the domain. Finally, the corner u_a values (i.e., u_a (1,1), u_a (1,63), u_a (64,1), u_a (64,63)) are set equal to the nearest interior u_a values and the vertical component of the advection current is assumed to be zero along the open boundary of the 63 X 63 grid. This allows the horizontal components of the advection current to be calculated from continuity along the outer boundary.

H. CALCULATION OF THE ADVECTION CURRENT

The ocean current used to advect the temperature and salinity fields in the forecast model is given by

$$u_a = u_e + u_g^* \quad ,$$

$$v_a = v_e + v_g^* \quad ,$$

and

$$w_a = w_e \quad , \tag{22}$$

where u_e, v_e, and w_e are the x-, y-, and z-components of the wind-driven Ekman circulation and u_g^* and v_g^* are the x- and y-components of a nondivergent geostrophic velocity field determined from a climatological data base.

1. Ekman Component of the Advection Current

Only the steady component of the wind-driven Ekman current which is in balance with the wind stress and the mixed-layer depth is used for advection. The time-dependent Ekman current calculated as part of the mixed-layer model (Equations 3 and 4) is not used in order to filter out inertial oscillations. Because of their periodic nature, inertial oscillations are not very effective in advecting the density field over distances on the scale of the model grid which has a resolution of 200 to 400 km. For example, the diameter of a 20 cm s^{-1} inertial current circle at 30°N is only 17 km. Filtering the inertial fluctuations from the Ekman current allows the use of a large time step for advection and a consequent saving of computer time. The advection terms are updated every 6 hours during the forecast, which is often enough to resolve changes in the wind field, but not often enough to resolve inertial oscillations without introducing noise into the horizontal and vertical advection fields.

The wind-driven Ekman current is calculated using the equations

$$0 = fv_e + \frac{\partial}{\partial z}\left(\overline{-w'u'} + \nu\frac{\partial u_e}{\partial z}\right) - Du_e \tag{23}$$

and

$$0 = -fu_e + \frac{\partial}{\partial z}\left(\overline{-w'v'} + \nu\frac{\partial v_e}{\partial z}\right) - Dv_e \ , \tag{24}$$

where the symbols have the same meanings defined previously.

The boundary conditions for these equations are that the surface stress is equal to the wind stress and that the stress at the base of the mixed layer ($z = -h$) is zero:

$$\left[\overline{w'u'} - \nu\frac{\partial u_e}{\partial z}\right]_{z=0} = \frac{-\tau^x}{\rho_w}, \tag{25}$$

$$\left[\overline{w'v'} - \nu\frac{\partial v_e}{\partial z}\right]_{z=0} = \frac{-\tau^y}{\rho_w}, \tag{26}$$

$$\left[\overline{w'u'} - \nu\frac{\partial u_e}{\partial z}\right]_{z=-h} = 0 \ , \tag{27}$$

and

$$\left[\overline{w'v'} - \nu\frac{\partial v_e}{\partial z}\right]_{z=-h} = 0 \ , \tag{28}$$

The zero stress condition at the base of the mixed-layer is a good approximation, since turbulent mixing in this region is almost completely suppressed by the stratification and the stress is quite small there relative to the mean stress within the mixed-layer.

The surface wind stress and the mixed-layer depth are required to define the boundary conditions. Forecast values of the wind stress are provided by FLENUMOCEANCEN atmospheric models (as discussed in Section II.G) and the mixed-layer depth is obtained from TOPS itself.

As in the mixed-layer equations, the Mellor-Yamada Level-2 turbulence closure scheme, described in Section II.C, is used to parameterize the

turbulent momentum fluxes $\overline{w'u'}$ and $\overline{w'v'}$. However, for the calculation of the steady Ekman advection current, the mixed-layer is taken to be completely mixed (i.e., unstratified with a Richardson number of zero). Hence, the momentum fluxes are a function only of the vertical shear of the horizontal velocities u_e and v_e.

Equations (23) and (24) are solved successively for each column of the grid at the T-S points (see Fig. 5). The Ekman velocities u_e and v_e are then horizontally interpolated to the points where the advection velocities u_a and v_a are defined. The vertical grid used is as described in Section II.E. As an initial guess to the Ekman velocity profiles, (23) and (24) are solved directly by setting the vertical eddy diffusion coefficient for momentum equal to 50 $cm^2\ s^{-1}$. The time dependent forms of (23) and (24) (see Equations (3) and (4)) are then integrated with a one-hour time step to convergence, with the eddy coefficients being updated each time step using the Mellor-Yamada turbulence parameterization.

The vertical motion that results from the horizontal divergence of the Ekman current field is calculated by integrating the continuity equation

$$\frac{\partial u_e}{\partial x} + \frac{\partial v_e}{\partial y} + \frac{\partial w_e}{\partial z} = 0 \tag{29}$$

from the surface to a depth z giving

$$w_e(z) = \int_z^0 \frac{\partial u_e}{\partial x} + \frac{\partial v_e}{\partial y}\, dz\,. \tag{30}$$

The vertical velocity at the surface has been taken to be zero. In actual calculations, w_e is defined at the same points as w_a (see Section II.E).

The vertical motion just below the mixed-layer due to the divergence of the surface Ekman current is sometimes referred to as the Ekman pumping or Ekman suction velocity. By substituting the steady Ekman equations into the continuity equation (29) and ignoring the drag terms (which are small) we can obtain

$$\rho_w w_e(-h) = \left(\frac{\tau^y}{f}\right)_x - \left(\frac{\tau^x}{f}\right)_y = \mathrm{curl}\left(\frac{\vec{\tau}}{f}\right). \tag{31}$$

In Equation (31), the Ekman pumping velocity w_e (-h) depends only on the wind stress curl and to a lesser extent on the latitudinal variation of the Coriolis parameter f. It is notable that the rate of Ekman pumping does not depend upon the particular parameterization used for turbulent mixing or the mixed-layer depth, and is therefore independent of the mixed-layer model itself.

2. Geostrophic Component of the Advection Current

The geostrophic currents used for advection are calculated from the FLENUMOCEANCEN climatological temperature and salinity fields. These fields are monthly averages and are available on the FLENUMOCEANCEN 63 X 63 Northern Hemisphere Polar Stereographic Grid used by TOPS at standardized depths from the surface to 5000 m.

Consideration was given to using the daily ocean thermal structure analysis to calculate the geostrophic advection currents. However, a trial calculation in which the climatological temperature field in the upper 400 m was replaced by the current OTS analysis resulted in a significant weakening of certain currents compared to the climatological calculation. Although the mid-latitude

currents such as the Gulf Stream and Kuroshio looked similar, the equatorial current system in the Pacific was severely diminished. The reason for this difference is unclear, but it suggests that the sparse data input to the analysis in this region is insufficient to resolve the horizontal density gradients. Because of this problem, the climatological temperature field is presently being used to calculate the geostrophic component of the advection current.

The procedure for calculating the geostrophic component of the advection current is: (1) the density field is calculated from the appropriate monthly temperature and salinity fields, (2) geostrophic currents are calculated from the density field using the thermal wind relations and a reference level of no motion, and (3) a stream function-vorticity equation is solved to eliminate the horizontal divergence of the geostrophic current and to satisfy the lateral boundary condition of no flow across land-sea boundaries.

The density field is calculated from the monthly climatological temperature and salinity fields using a polynomial formulation of the equation of state for seawater developed by Friedrich and Levitus (1972). The densities are calculated at the T-S points of the grid where the climatological temperature and salinity fields are defined, and then horizontally interpolated to the corner points of the dashed-line boxes of Figure 5. This allows the geostrophic velocities to be directly calculated at the points where the advection velocities u_a and v_a are located.

The thermal wind equations are used to calculate the geostrophic current from the density field. These relations (given by Pond and Pickard, 1978) are

$$\frac{\partial u_g}{\partial z} = \frac{g}{\rho f} \frac{\partial \rho}{\partial y} \quad , \tag{32}$$

and

$$\frac{\partial v_g}{\partial z} = \frac{-g}{\rho f} \frac{\partial \rho}{\partial x} \quad . \tag{33}$$

The use of the above equations allows only the calculation of relative currents. In order to calculate absolute currents, the absolute velocity at some depth must be specified. An assumption frequently used is that, at a certain depth, the currents become small and can be taken to be zero. Such an assumption, when used to estimate current transports over a deep water column, can lead to significant errors, since deep currents can be large enough to yield appreciable transports when integrated over a large depth. Since deep currents tend to be much weaker than surface currents, however, the use of a depth of no motion to estimate upper-ocean currents generally yields reasonably small errors.

The reference level or level of no motion that was selected for calculating geostrophic currents from the climatological density fields is a function of latitude and is based on a number of trial calculations using reference levels between 400 and 2500 m. Below the equator (i.e., in the "corners" of the 63 X 63 northern hemisphere grid) the deep density climatology is extremely poor and a reference level of 500 m is used. The use of a deeper reference level in this region generates spurious currents. Above 30°N a reference level of 1250 m is used. The strongest currents in this region, the Gulf Stream and the Kuroshio, have depth scales of about 1000 m. These currents are not much enhanced by using a deeper reference level, but are significantly reduced when the reference depth is

decreased. Between 0°N and 30°N the reference depth was arbitrarily taken to be a linear function of latitude to provide a smooth transition of the level of no motion between these two latitudes. It was found that the equatorial currents calculated from the climatological density fields between 0°N and 30°N are relatively shallow and are not sensitive to the depth of the reference level as long as it is greater than about 400 m. The use of a reference level for the calculation of geostrophic currents that increases with latitude is consistent with the findings of previous investigators. For example, Defant (1941) found the optimum reference level to be about 600 m near the equator, increasing to 1250-2000 m at 40°N in the Atlantic.

A problem occurs when applying the thermal wind equations near the equator where f approaches zero. Although the geostrophic approximation is considered to be fairly good to within one or two degrees of the equator, small errors in the density field near the equator can generate large spurious currents. For this reason, the value of f used for calculating the geostrophic current in the region between 5°N and 5°S is taken to be

$$f = f \text{ (at } 5^{o}N) \text{ for } 0^{o} \leq \text{latitude} \leq 5^{o}N \quad ,$$

and (34)

$$f = f \text{ (at } 5^{o}S) \text{ for } 5^{o}S \leq \text{latitude} < 0^{o} \quad .$$

This treatment yields a realistic looking equatorial current system.

It is desirable to eliminate the horizontal divergence of the geostrophic component of the advection current. Since calculating divergence involves taking a small difference between large terms, small errors in the horizontal current (due to noise in the density field) tend to cause large errors in the vertical motion field, which is calculated from the divergence of the horizontal geostrophic current. Since the geostrophic current is calculated from monthly climatology, erroneous features in the vertical motion field will persist for at least a month until this field is updated. It TOPS is used for long forecasts, or if the model forecast is fed back into the daily ocean thermal structure analysis, these persistent errors in the vertical advection field could have cumulative effects that would generate significant errors in the predicted and analyzed density fields.

In order to eliminate the horizontal divergence of the geostrophic velocity field, a stream function-vorticity equation is solved at each level. This equation is given by

$$\frac{\partial^2 \psi}{\partial x^2} + \frac{\partial^2 \psi}{\partial y^2} = \frac{\partial v_g}{\partial x} - \frac{\partial u_g}{\partial y} \quad , \tag{35}$$

where the right-hand-side of the above equation is the vertical component of vorticity of the divergent geostrophic velocity field and ψ is the stream function. A horizontally non-divergent velocity field is obtained from the stream function using the standard definitions

$$u_g^* = - \frac{\partial \psi}{\partial y} \quad , \tag{36}$$

and

$$v_g^* = \frac{\partial \psi}{\partial x} \quad . \tag{37}$$

Here, the velocity field defined from the stream function is designated by an asterisk to differentiate it from the divergent geostrophic field that appears on the left-hand-side of (32) and (33).

The stream function is defined at the corners of the dashed-line boxes shown in Figure 5. On the land-sea boundaries, the stream function is set to zero so that there will be no flow across these boundaries. The single exception is that the stream function on the Cuba-Haiti island group is defined to be (1 - depth/1000 m) x $5X10^4$ m^2 s^{-1} to provide a transport of 25 Sverdrups (25 X 10^6 m^3 s^{-1}) through the Yucatan and Florida Straits. Since the Florida Straits span only one grid interval, this is the simplest means of getting a reasonable flow through this region.

Boundary conditions along the open boundaries of the grid which span the South Atlantic, the South Pacific, and the Indian Ocean (see Figure 4) are defined by normalizing the geostrophic transport across each of these boundaries to zero by means of an additive constant. The normalization of the transport across the open boundaries has the effect of distorting the flow near some parts of the boundary. This distortion is most severe along the South Atlantic boundary because the near-surface geostrophic flow across this boundary is almost entirely northward. However, the distortion diminishes significantly within 10 to 20° of the boundary.

Equation (35) is solved for the stream function at each level using successive-over-relaxation. Because the model grid is relatively coarse, the solution converges sufficiently in just a few iterations.

III. SUMMARY AND OUTLOOK

The Thermodynamical Ocean Prediction System (TOPS) is a general and flexible software framework for operational implementation of upper ocean forecast models at Fleet Numerical Oceanography Center (FLENUMOCEANCEN). It was developed by NORDA Code 322 as a part of the Navy's Automated Environmental Prediction System (AEPS). TOPS is fully interfaced with the FLENUMOCEANCEN operational data base and meets all FLENUMOCEANCEN programming standards for operational programs.

The horizontal grid used by TOPS is the standard FLENUMOCEANCEN 63 X 63 Northern Hemisphere Polar Stereographic Grid. The vertical grid consists of 17 levels between the surface and 500 m depth with stretching employed to retain high resolution in the upper 100 m for proper treatment of the mixed-layer.

TOPS is initialized by the daily FLENUMOCEANCEN analysis of ocean thermal structure and a daily interpolation of monthly climatological salinity fields. The ocean predictions are driven out to a forecast time of 72 hours by fluxes of heat, moisture and momentum at the sea surface supplied by operational FLENUMOCEANCEN atmospheric models.

Two forecast models are available in the system. In the non-advective model, the time rate of change of temperature and salinity is due only to the convergence of vertical eddy and radiative fluxes. Thus, even though the model produces a three-dimensional forecast of the upper ocean, it contains only one-dimensional physical processes and is, therefore, termed a "quasi-one-dimensional" model. In the advective model, horizontal and vertical advection and horizontal diffusion of temperature and salinity are included in addition to the radiative and vertical

mixing processes of the non-advective model. The horizontal pressure gradient term is still not included in the equations of motion; therefore, the model cannot be used to determine the geostrophic component of the flow. Thus, even though advection and diffusion of temperature and salinity occur in three dimensions in this formulation, it is not a true three-dimensional model and is therefore termed a "quasi-three-dimensional" model.

In the present configuration of the advective model, the geostrophic component of the advection current is calculated diagnostically from a climatological data base. The Ekman component of the advection current is determined from the predicted local values of mixed layer depth and surface wind stress.

In both models, the Level-2 turbulence closure theory of Mellor and Yamada (1974) is used to parameterize the vertical eddy fluxes of heat, salinity, and momentum. The basic assumption of this parameterization is that the turbulent kinetic energy budget at each level in the mixed-layer consists of a balance between shear production, buoyancy production and viscous dissipation.

The advective model will be installed on the CYBER 203 computer at FLENUMOCEANCEN in 1981 and will become the primary operational model in TOPS. The non-advective model is currently operative on the CYBER 175 at Monterey, and even after the advective model becomes operational, will remain active by serving as a back-up model to be run on the CYBER 175 in the event that the CYBER 203 is down. This back-up capability is important in an operational context and will help guarantee the daily availability of the product fields generated by TOPS.

Since the thermodynamical structure of the upper ocean has important implications for many activities, there are multiple uses for TOPS. From the Navy's viewpoint, however, the uses for TOPS are mainly twofold: (1) improve the daily analysis of upper ocean thermal structure by generating 24-hour forecasts for use as first-guess fields in the analysis, and (2) provide real-time 72-hour forecasts of tactically significant changes in the thermal structure of the mixed-layer.

From a software standpoint, TOPS has been designed in a highly modular fashion. This will allow the system to undergo continual evolution with relative ease. In future applications, for example, TOPS will be coupled with a hydrodynamical model (presently under development by NORDA Code 322) that will supply geostrophic advection currents that are more dynamically consistent than those now used. Since proper treatment of hydrodynamical processes requires adequate representation of mesoscale eddies and, hence, extremely high horizontal resolution, the hydrodynamical model will necessarily have coarse vertical resolution. Thus, although the hydrodynamical component of this coupled hybrid-system will have coarse vertical resolution, the thermodynamical component will retain fine vertical resolution in order to allow proper representation of thermodynamical processes and provide meaningful input to acoustic models. Furthermore, zoomed (i.e., limited area, fine horizontal resolution) versions of the system may be produced to complement the zoomed versions of the daily ocean thermal structure analysis that are available. In addition, more sophisticated turbulence parameterization models may eventually be utilized.

At all stages in the development of operational forecast systems, forecast verification must play a significant role. Although the turbulence parameterization scheme currently used in the system (which forms the heart of the forecast models) has been tested successfully in a number of one-dimensional

studies by several authors (see Section II.C), it is still quite necessary to test the overall forecast system. This is true mainly because (1) TOPS depends on the FLENUMOCEANCEN operational data base for initial conditions and surface forcing; consequently, its value is closely linked to the quality of this data, (2) performing in operational mode, the turbulence model will be subjected to a range of conditions wider than what was considered in the one-dimensional studies, and (3) in the advective model, three-dimensional processes are also included.

During the developmental stage, informal and limited test and evaluation studies were conducted on TOPS by NORDA personnel with very encouraging results. Formal and extensive test and evaluation programs on the present and future versions of TOPS will be carried out primarily by FLENUMOCEANCEN personnel and represent important steps before the various models can achieve full operational status.

Quantitative verification of a large-scale ocean forecast poses special problems because of the nonuniform and constantly changing spatial distribution of the limited number of daily-available XBT and sea-surface temperature observations. Meaningful forecast verification can be accomplished only in data-rich regions, since the model forecast will probably be more realistic than the subsequent analysis in data-sparse regions. This is the case because the forecast model will respond to the atmospheric forcing in a dynamically consistent way everywhere, while the analysis will simply remain near the climatological state in data-sparse regions, regardless of the local atmospheric forcing. Thus, when these test and evaluation programs are performed, the distribution of the various observations must be monitored on a day-by-day basis. This will allow subregions of the grid that have adequate data coverage at both the beginning and end of a forecast period to be identified. Model forecasts in these subregions can then be quantitatively compared to forecasts of persistence and climatology, with the daily analysis at the end of the forecast period providing the verification data (the model forecast would not be used to generate the first-guess field for the analysis in these comparisons). Finally, when evaluating an ocean prediction system in this way, the relative contribution of the three primary sources of apparent forecast error, (1) improper initial conditions, (2) inaccurate atmospheric forcing, (3) imperfect representation of oceanic dynamics and (4) inexact verification data, must be sorted out.

IV. REFERENCES

Camp, N.T. and R.L. Elsberry (1978). Oceanic Thermal Response to Strong Atmospheric Forcing II. The Role of One-Dimensional Processes. J. Phys. Oceanog., 8, 215-224.

Clancy, R.M. (1979). A Model of Diurnal Variability of the Ocean-Atmosphere System in the Undisturbed Trade Wind Regime. Tech. Report SAI-79-807-WA, Science Applications, Inc., 8400 Westpark Drive, McLean, VA, July, 114 p.

Defant, A., (1941). Die Absolute Topographic des Physikalishen Meersniveaus and der Druckflächen, Sowie die Wasserbewegungen im Atlantischen Ozean. Meteor-Werk, 6, No. 2, Liefg. 5, 191-260.

Elsberry, R.L. and N.T. Camp (1978). Oceanic Thermal Response to Strong Atmospheric Forcing I. Characteristics of Forcing Events. J. Phys. Oceanog., 8, 206-214.

Elsberry, R.L. and S.D. Raney (1978). Sea Surface Temperature Response to Variations in Atmospheric Wind Forcing. J. Phys. Oceanog., 8, 881-887.

Elsberry, R.L., P.C. Gallacher, and R.W. Garwood (1979). One-Dimensional Model Predictions of Ocean Temperature Anomalies During Fall 1976. Tech Report NPS 63-79-003, Naval Postgraduate School, Monterey, CA, August, 30 p.

Freidrich, H., and S. Levitus (1972). An Approximation to the Equation of State for Sea Water, Suitable for Numerical Ocean Models. J. Phys. Oceanog., 2, 514-517.

Holl, M.M., M.J. Cuming, and B.R. Mendenhall (1979). The Expanded Ocean Thermal-Structure Analysis System: A Development Based on the Fields by Information Blending Methodology. Tech. Report M-241, Meteorology International Incorporated, 205 Montecito Avenue, Monterey, CA, July, 216 p.

Jerlov, N.G. (1968). Optical Oceanography. New York, Elsevier, 352 p.

Johnson, W.F. (1977). Upper Ocean Thermal Structure Forecast Evaluation of a Model Using Synoptic Data. M.S. Thesis, Naval Post Graduate School, Monterey, CA, 47 p.

Martin, P.J. (1976). A Comparison of Three Diffusion Models of the Upper Mixed Layer of the Ocean. NRL Memorandum Report 3399, Naval Research Laboratory, Washington, DC, 62 p.

Martin, P.J. and G.O. Roberts (1977). An Estimate of the Impact of OTEC Operation on the Vertical Distribution of Heat in the Gulf of Mexico. Proc. of 4th OTEC Symposium, P. IV-26, G. Ioup. (ed 1).

Martin, P.J. and G.O. Roberts (1978). Peak Current Profile Estimates at Selected Sites for Ocean Thermal Energy Conversion. SAI Tech. Report, Science Applications, Inc., 8400 Westpark Drive, McLean, VA.

Martin, P.J. and J.D. Thompson (1980). Formulation and Testing of a Layer-Compatible Upper Ocean Mixed-Layer Model. Paper submitted to Journal of Physical Oceanography.

Mellor, G.L. and T. Yamada (1974). A Hierarchy of Turbulence Closure Models for Planetary Boundary Layers. J. Atmos. Sci., 31, 1791-1806.

Mellor, G.L. and P.A. Durbin (1975). The Structure and Dynamics of the Ocean Surface Mixed Layer. J. Phys. Oceanog., 5, 718-725.

Niiler, P.P. and E.B. Kraus (1977). One-Dimensional Models of the Upper Ocean. Chapt. 10, Modelling and Prediction of the Upper Layers of the Ocean. New York, Pergamon Press, 325 p. (Pergamon Marine Series, v. 1).

Paulus, R.A. (1978). Salinity Effects in an Oceanic Mixed-Layer Model. M.S. Thesis, Naval Post Graduate School, Monterey, CA, 77 p.

Pollard, R.T. and R.C. Millard (1970). Comparison Between Observed and Simulated Wind-Generated Inertial Oscillations. Deep Sea Res., 17, 813-821.

Pond, S. and G.L. Pickard (1978). Introductory Dynamic Oceanography. New York, Pergamon Press, 241 p.

Warn-Varnas, A.C. and S.A. Piacsek (1979). An Investigation of the Importance of Third-Order Correlations and Choice of Length Scale in Mixed Layer Modelling. Geophys. Astrophys. Fluid Dyn., 13, 225-243.

Warn-Varnas, A.C., G.M. Dawson, P.J. Martin, and M. Miyake (1980). Forecasts and Studies of the Oceanic Mixed Layer During the MILE Experiment. Paper Submitted to Journal of Geophysical and Astrophysical Fluid Dynamics.

Weigle, W. F. and B. R. Mendenhall (1974). Climatology of the Upper Thermal-Structure of the Seas. Tech. Report M-196, Meteorology International, Incorporated, 205 Montecito Avenue, Monterey, CA, 79 p.

APPENDIX

LIST OF SYMBOLS

APPENDIX

LIST OF SYMBOLS

SYMBOL	DEFINITION
A	Horizontal eddy diffusion coefficient.
B_o	Upward infrared radiation flux at sea surface.
c	Specific heat of seawater.
C_D	Drag coefficient for surface wind stress calculation.
D	Damping coefficient for inertial oscillations.
F	Downward flux of solar radiation.
F_o	Downward flux of solar radiation at sea surface.
f	Coriolis parameter.
g	Acceleration of gravity.
h	Thickness of mixed layer.
H_o	Upward sensible heat flux at sea surface.
I	Downward flux of solar radiation at sea surface scaled by the cosine of the local zenith angle.
K_H	Vertical eddy diffusion coefficient for heat and salinity.
K_M	Vertical eddy diffusion coefficient for momentum.
ℓ	Turbulence length scale.
L	Latent heat of evaporation for water.
P_o	Surface precipitation rate.
q	The square root of twice the turbulent kinetic energy.
Q_o	Upward evaporative flux of moisture at sea surface.
Ri	Gradient Richardson number.
S	Salinity.
S_o	Salinity at sea surface.
S_H	Stability function for vertical eddy fluxes of heat and salinity.
S_M	Stability function for vertical eddy flux of momentum.

t	Time.
T	Temperature.
u	x-component of current velocity.
u_e	x-component of steady Ekman part of advection current.
u_g	x-component of geostrophic current.
u_g^*	x-component of divergence-free geostrophic part of advection current.
u_a	x-component of advection current.
U	x-component of wind velocity at reference height above sea surface.
v	y-component of current velocity.
v_e	y-component of steady Ekman part of advection current.
v_g	y-component of geostrophic current.
v_g^*	y-component of divergence-free geostrophic part of advection current.
v_a	y-component of advection current.
V	y-component of wind velocity at reference height above sea surface.
w	z-component of current velocity.
w_e	Ekman-induced z-component of current velocity.
w_a	z-component of advection current.
x	Grid-referenced horizontal coordinate (see Fig. 4).
y	Grid-referenced horizontal coordinate (see Fig. 4).
z	Vertical coordinate, positive upward from sea surface.
$(\bar{\ })$	Spatial average at constant depth taken over region defined by grid cell of horizontal grid.
$(')$	Departure from above-defined spatial average.
α	Local zenith angle of the sun.
γ	Fraction of surface flux of solar radiation pentrating to a depth z.
ν	Background vertical eddy diffusion coefficient.

ρ	Density of seawater.
ρ_a	Reference density for air.
ρ_w	Reference density for water.
ψ	Stream function.
τ^x	x-component of surface wind stress vector.
τ^y	y-component of surface wind stress vector.
$\bar{\tau}$	Surface wind stress vector.

UNCLASSIFIED

SECURITY CLASSIFICATION OF THIS PAGE (When Data Entered)

REPORT DOCUMENTATION PAGE		READ INSTRUCTIONS BEFORE COMPLETING FORM
1. REPORT NUMBER NORDA Technical Note 54	2. GOVT ACCESSION NO.	3. RECIPIENT'S CATALOG NUMBER
4. TITLE (and Subtitle) The NORDA/FLENUMOCEANCEN Thermodynamical Ocean Prediction System (TOPS): A Technical Description		5. TYPE OF REPORT & PERIOD COVERED 6. PERFORMING ORG. REPORT NUMBER
7. AUTHOR(s) R. Michael Clancy Paul J. Martin		8. CONTRACT OR GRANT NUMBER(s)
9. PERFORMING ORGANIZATION NAME AND ADDRESS Naval Ocean Research and Development Activity NSTL Station, Mississippi 39529		10. PROGRAM ELEMENT, PROJECT, TASK AREA & WORK UNIT NUMBERS
11. CONTROLLING OFFICE NAME AND ADDRESS Naval Ocean Research and Development Activity Numerical Modeling Division NSTL Station, Mississippi 39529		12. REPORT DATE November 1979 13. NUMBER OF PAGES 31
14. MONITORING AGENCY NAME & ADDRESS(if different from Controlling Office)		15. SECURITY CLASS. (of this report) Unclassified 15a. DECLASSIFICATION/DOWNGRADING SCHEDULE
16. DISTRIBUTION STATEMENT (of this Report) Unlimited		
17. DISTRIBUTION STATEMENT (of the abstract entered in Block 20, if different from Report)		
18. SUPPLEMENTARY NOTES		
19. KEY WORDS (Continue on reverse side if necessary and identify by block number) Ocean forecast model Ocean thermal structure Oceanic mixed layer Ocean circulation		

20. ABSTRACT (Continue on reverse side if necessary and identify by block number)

The Thermodynamical Ocean Prediction System (TOPS) is a general and flexible software framework for operational implementation of upper ocean forecast models at Fleet Numerical Oceanography Center (FLENUMOCEANCEN). It was developed by NORDA Code 322, Numerical Modeling Division, as a part of the Navy's Automated Environmental Prediction System (AEPS). This technical note discusses the uses for TOPS, provides documentation of the physics currently implemented in the system, indicates probable future developments and briefly addresses the problem of forecast verification.

DD FORM 1 JAN 73 1473 EDITION OF 1 NOV 65 IS OBSOLETE

UNCLASSIFIED